SECOND EUROPEAN CONFERENCE ON EARTHQUAKE ENGINEERING
AND SEISMOLOGY, ISTANBUL AUG. 25-29, 2014

MODAL IDENTIFICATION AND DAMAGE ESTIMATION FOR HEAVILY DAMAGED NINE-STORY SRC BUILDING BY AMBIENT VIBRATION MEASUREMENTS

Kahori IIYAMA[1] , Satoshi KURITA[2] , and Masato MOTOSAKA[3]

ABSTRACT

The development of methods for modal identification and damage detection is important to structural health monitoring. However, studies based on measuring structures actually affected by huge earthquakes have been limited. In this study, the modal parameters of a heavily damaged nine-story steel-reinforced concrete (SRC) building were identified based on high-density array measurements of ambient vibrations. The three-dimensional mode shapes, torsional vibration characteristics, slope of the mode shape, and changes in the natural frequency over time were demonstrated, and the relationship between these characteristics and the damage location was considered.

INTRODUCTION

In recent years, structural health monitoring has attracted attention and extensive studies on structure assessment and damage identification have been presented. Among these studies, a lot of approaches focusing on modal parameters have been introduced and demonstrated the efficacy of their methods (e.g., Yang and Nagarajaiah, 2013, Xu and Wu, 2012, Au and Zhang, 2011, Kim, 2002, and Teughels et al., 2002). Meanwhile, Nakamura and Yasui (1999) assessed story stiffness on actual buildings before and after damage and pointed out the importance of three-dimensional characteristics for error reduction on damage identification. Hamamoto and Kondo (1999) proposed damage detection (DD) method which utilizes torsional modes, and demonstrated the validity of the method by a laboratory test. Ghahari et al. (2013) also mentioned that the contribution of torsional mode might cause inaccuracies in estimating the translational mode. These results indicate availability of three-dimensional vibrational characteristics for damage detection; however, studies focused on the three-dimensional characteristics of severely damaged buildings have been limited. Although laboratory tests and measurements using large-scale structure has been performed in recent studies (e.g. Belleri et al, 2014, Hsu and Loh, 2013, Omrani et al., 2012, Moaveni et al., 2010, Strauss et al., 2010), further information on the detailed vibration characteristics of actual structures needs to be collected.

In this study, the ambient vibrations of a nine-story SRC building that was heavily damaged by the 2011 Tohoku earthquake were measured by using a high-density array. The building's modal properties were identified through frequency domain decomposition (FDD), which is an output-only technique. Based on the identified modal parameters, the three-dimensional mode shapes, torsional deformation, distribution patterns of the slope of the mode shape, and the changes in natural frequency

[1] Assistant Professor, Tokyo University of Science, Tokyo, kiiyama@rs.kagu.tus.ac.jp
[2] Professor, Tokyo University of Science, Tokyo, kurita@rs.kagu.tus.ac.jp
[3] Professor, Tohoku University, Sendai, motosaka@irides.tohoku.ac.jp

for the first-order modes over time were evaluated. The relation between these characteristics and the damage condition was examined.

OBJECTIVE BUILDING

The objective building was a nine-story SRC building belonging to Tohoku University in Sendai, Japan (Photo 1a). It was constructed in 1969 on a pile foundation with moment-resistant frames and shear walls. The structure consisted of a 32.9 m tall nine-story building and two-story pilotis along both sides of the building (Fig. 1). The earthquake-resistant elements were mainly allocated to the north side of the floors, as shown by the floor plans for the initial building design in Figs. 1a and b. Thus, the stiffness distribution of the building was unbalanced in the longitudinal direction in the initial design.

Since 1969, the building often experienced major earthquakes. In particular, the 1978 Miyagi-ken Oki earthquake (magnitude 7.4) heavily damaged the bottom of four corner columns and the side shear walls (Tsamba and Motosaka, 2011). The building was once retrofitted from September 2000 over six months. Four retrofits were performed as shown in Fig. 2 (Motosaka et al., 2002): replacement of concrete side walls, installation of steel braces, reinforcement of beams by steel plate wraps, and reinforcement of floor slabs. Based on the design values of the seismic retrofitting, Hirabayashi et al. (2012) demonstrated that the eccentricities of the center of stiffness were small enough on each floor in both the longitudinal and transversal directions. This means that the unbalanced stiffness distribution in the longitudinal direction of the initial design was reduced after the seismic retrofitting. However, the 2011 Tohoku earthquake crushed the four corner columns and shear walls on the third floor by rocking vibrations (Photo 1b). A peak horizontal acceleration of 908 Gals was observed on the ninth floor. Approximately two months after the earthquake, emergency rehabilitation was conducted on the third floor so that people could carry furniture and materials out of the building safely. The four corner columns were strengthened by adding RC jackets with steel rods in the axial direction, and reinforced concrete shear walls were installed in the longitudinal corner frames (Photo 1c).

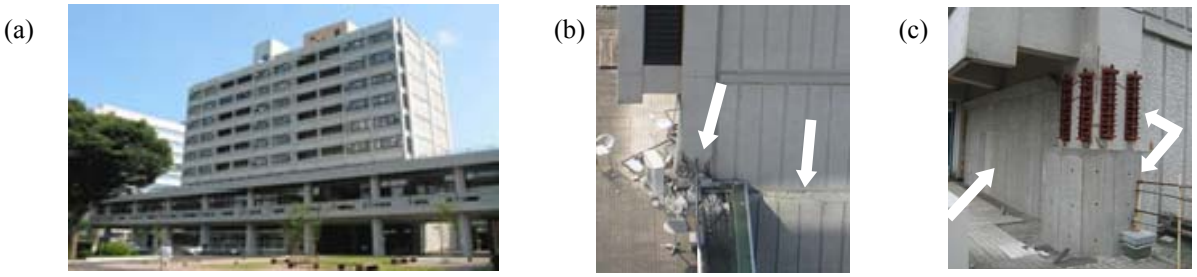

Photo 1. (a) Objective building, (b) crushed column, and (c) emergency rehabilitation

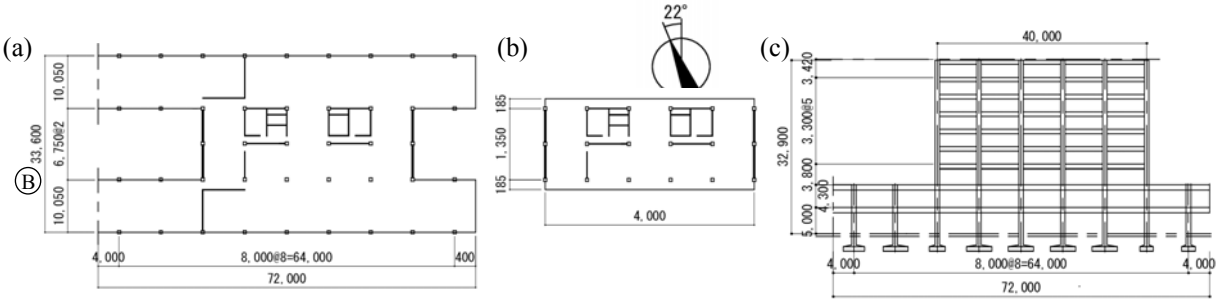

Figure 1. Plan of objective building : (a) second floor plan, (b) typical floor plan, and (c) line-B plan

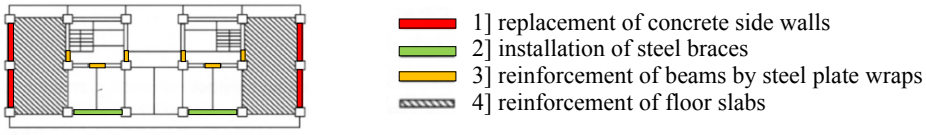

Figure 2. Seismic retrofitting from September 2000 over six months (Motosaka et al., 2002)

METHODOLOGY

An output-only algorithm was applied to modal identification of the building. FDD proposed by Brincker et al. (2001) is a simple and useful technique based on the theory of a non-proportional damping vibration system. In this study, the FDD technique proposed by Iiyama and Kurita (2013) was used. The techniques are briefly given below.

Let $\{Y\}$ be a column vector representing the Fourier transforms of the N measured responses; then the output spectral density matrix $[G]$ can be defined as follows:

$$[G(j\omega)] = E[\{\overline{Y}(j\omega)\}\{Y(j\omega)\}^T] \tag{3.1}$$

where ω is the circular frequency, j denotes an imaginary unit, $E[\ ]$ denotes the ensemble average, index $^-$ denotes a complex conjugate, and superscript T denotes transposition. The output spectral density matrix can be decomposed by singular value decomposition into singular values $s_i(j\omega)$ and singular vectors $\{U_i(j\omega)\}$. Around the rth mode (reference mode) frequency ω_r, only the first singular value $s_1(j\omega)$, which has the maximum value among $s_i(j\omega)$ ($i = 1,\ldots, N$), dominates and has a peak at $\omega = \omega_r$. Then, the following approximation holds:

$$[\overline{G}(j\omega)] = \sum_{i=1}^{N} s_i(j\omega)\{U_i(j\omega)\}\{U_i(j\omega)\}^H \approx s_1(j\omega)\{U_1(j\omega)\}\{U_1(j\omega)\}^H \tag{3.2}$$

where superscript H denotes a complex conjugate and transpose and $\{U_1(j\omega)\}$ is the first singular vector. Brincker et al. (2001) introduced the following approximation of $[G]$ around $\omega = \omega_r$ under a non-proportional damping system subjected to white noise excitation:

$$[\overline{G}(j\omega)] \approx a_r(j\omega)\{\phi_r\}\{\phi_r\}^H \ , \quad a_r(j\omega) = \mathrm{Re}\left(\frac{2d_r}{j\omega - \lambda_r}\right) \tag{3.3}$$

where d_r is a constant value relevant to white noise excitations and $\{\phi_r\}$ is the rth complex mode shape vector of the system. λ_r is the pole represented by the sum of the rth modal damping ratio σ_r and rth damping circular frequency ω_{dr}: $\lambda_r = -\sigma_r + j\omega_{dr}$. Considering the correspondence between Eqs. (3.2) and (3.3), the eigen-frequency is ω_r, which shows one of the peaks for $s_1(j\omega)$, and the ith eigenmode is identified as $U_1(j\omega_r)$. In addition, the modal damping factor h_r is simply estimated from the SDOF autocorrelation function obtained by performing an inverse Fourier transform on $s_1(j\omega)$ around $\omega = \omega_r$.

Iiyama and Kurita (2013) reconstructed the technical background of FDD and approximated $[G]$ to determine the influence of existing sth modes ($s \neq r$) on the identification accuracy of rth modal parameters. Based on the background, they proposed using the real part of $[G]$ to identify the modal parameters for a proportional damping system. Similar to Eq. (3.2), the real part of $[G]$ can be decomposed by spectral decomposition and approximated by

$$[G^R(j\omega)] = \sum_{i=1}^{N} q_i(j\omega)\{p_i(j\omega)\}\{p_i(j\omega)\}^T \approx q_1(j\omega)\{p_1(j\omega)\}\{p_1(j\omega)\}^T \tag{3.4}$$

where superscript R represents the real part of a complex matrix and $q_i(j\omega)$ and $\{p_i(j\omega)\}$ are the ith eigenvalue and the corresponding eigenvector, respectively. The approximation of $[G^R]$ around the rth circular frequency ω_r subjected to white noise excitation is given by

$$[G^R(j\omega)] \approx 2a_{rr}^p(j\omega)\left(\{\phi_r\} + \{\Delta_r^p(j\omega)\}\right)\left(\{\phi_r\} + \{\Delta_r^p(j\omega)\}\right)^T \ ,$$

$$2a_{rr}^p(j\omega) = \frac{c_{rr}}{\sigma_r^2 + (\omega - \omega_{dr})^2} = a_r(j\omega) \tag{3.5}$$

where c_{rr} is a constant relevant to white noise excitation, $\{\phi_r\}$ is the rth real eigenmode of the system, and $\{\Delta_r^p(j\omega)\}$ is an error vector relevant to the existing close modes (Iiyama and Kurita, 2013). They demonstrated that $\{\Delta_r^p(j\omega)\}$ takes the smallest value at $\omega = \omega_{dr}$ and decreases the difference between ω_r and ω_s ($s \neq r$) increases. The procedures to identify the eigen-frequency, eigenmode, and modal damping are almost the same as those used by Brincker et al.

AMBIENT VIBRATION MEASUREMENT

(*i*) *Measurement conditions*

Simultaneous high-density array measurements of ambient vibrations were performed in September 2011 and January 2012. Thirty portable accelerometers were used: 26 GPL-6A3P sensors from Mitutoyo Co. and four JU210 sensors from Hakusan Co.. The accelerometers were set at three locations (NW, SW, NE) on each floor, as shown in Fig. 3. The ambient vibrations were recorded continuously for 45 or 60 min, at a sampling frequency of 200 Hz.

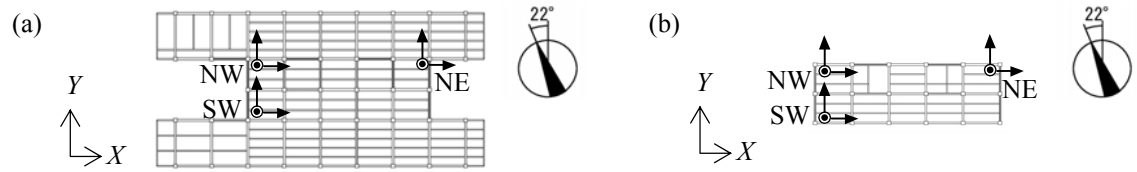

Figure 3. Location of accelerometers and indices: (a) first and second floors (lower floors), (b) floors above the second floor (upper floors)

(*ii*) *Time synchronization*

Although the inner clocks of the accelerometers were synchronized using a GPS system just before being set up at each location, the time delays of the clocks gradually progressed during the measurements. The relative time lags between measurement records can be estimated by using the cross spectral density function (CSDF) as follows. Assume that there are no time delays in time history $x(t)$ and that there is an average delay of τ_0 (s) in $y(t)$. The following equation can be obtained from the Fourier transform of $x(t)$ and $y'(t) = y(t-\tau_0)$ and the CSDF ($S_{XY'}$):

$$X(\omega) = \int_{-\infty}^{\infty} x(t)e^{-i\omega t}dt, \quad Y'(\omega) = \int_{-\infty}^{\infty} y(t-\tau_0)e^{-i\omega t}dt = e^{-i\omega\tau_0}Y(\omega) \tag{3.6}$$

$$S_{XY'}(\omega) = \overline{X}(\omega)\cdot Y'(\omega) = e^{-i\omega\tau_0}\overline{X}(\omega)\cdot Y(\omega) = \left|S_{XY}(\omega)\right| e^{i(\theta(f)-2\pi\tau_0 f)} \tag{3.7}$$

where $\theta(f)$ is the phase difference between $X(\omega)$ and $Y(\omega)$. Since the exponential part of Eq. (3.7) indicates the phase of $S_{XY'}$, the relative time lags emerge as a straight line with a slope of $-2\pi\tau_0$ on the phase. If there is no relative time lag between two sensors ($\tau_0 = 0$), the phases of $S_{XY'}$ are nearly equal to zero at low frequencies because floor slabs and columns may behave rigidly at frequencies lower than the first eigen-frequency. As an example, Fig. 4a shows the phases of $S_{XY'}$ between two sensors on the roof and on the eighth floor at location NE; the black and blue circles represent the phase differences in the longitudinal and up-down (UD) directions, respectively. In particular, the slope for the UD direction can clearly be seen for the frequency range of 2-10 Hz.

The optimal relative time lag τ_0 can be calculated by fitting the phases to $\theta(f) = 2\pi\tau_0 f$ by the least-squares method in the straight line frequency range. Fig. 4b shows the phases of $S_{XY'}$ after the time correction. The phases were nearly equal to zero at low frequencies.

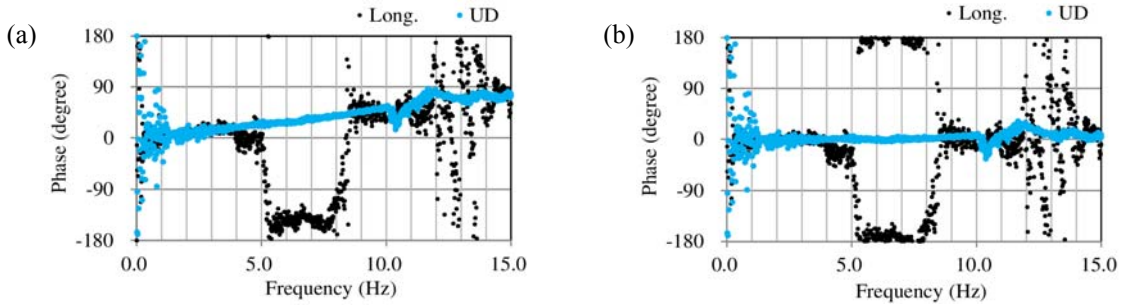

Figure 4. Phase of CSDF between two sensors: (a) before time correction and (b) after time correction

MODAL IDENTIFICATION

(*i*) *Frequency and mode shape*

The FDD technique was performed by using the absolute acceleration records after the time correction. The first eigenvalues are shown in Fig. 5. The peak frequencies of 1.43, 1.51, 2.23, 3.97, 4.96, and 6.71 Hz were considered; the corresponding eigenvectors are shown on the left side of Fig. 6 with respect to each location. Each eigenvector was normalized where the maximum value was 1.0. The three-dimensional modes shown on the right side of Fig. 6 were created from the modes of each floor at the center of mass, represented by the mode vector $\{u_X^C, u_Y^C, u_R^C\}^T$, where subscript *X*, *Y* and *R* denote the *X*-, *Y*- and rotational-directions. The coordinate of the center of mass represented by (X_c, Y_c) was allocated as shown in Fig.7 in this study. The mode vector $\{u_X^C, u_Y^C, u_R^C\}^T$ was converted from the identified modes represented by $\{u_X^j, u_Y^j\}^T$, where subscript *j* denotes the location number. The vector $\{u_X^j, u_Y^j\}^T$ indicates the mode at each location (X_j, Y_j) which corresponds to the eigenvector shown on the left side of Fig. 6. Then, the square error *J* of the difference between the identified modes $\{u_X^j, u_Y^j\}^T$ and the converted mode $\{u_X^C, u_Y^C, u_R^C\}^T$ under the assumption of a rigid floor slab is obtained by

$$J(u_X^C, u_Y^C, u_R^C) = \sum_{j=1}^{N_m} \left[\left\{ (u_X^C - (Y_j - Y_c) u_R^C) - u_X^j \right\}^2 + \left\{ (u_Y^C + (X_j - X_c) u_R^C) - u_Y^j \right\}^2 \right] \tag{3.8}$$

where N_m is the number of measurement points on each floor. The mode values $\{u_X^C, u_Y^C, u_R^C\}^T$ were determined by minimizing the error *J*. In this study, the calculated *J* was almost less than 1% of the following J_0 except for the mode VI. This indicates that the floor slabs can be considered to be sufficiently rigid during translational motion at low frequencies.

$$J_0(0,0,0) = \sum_{j=1}^{3} \left\{ (u_X^j)^2 + (u_Y^j)^2 \right\} \tag{3.9}$$

According to Fig. 6, mode I (1.43 Hz) was the first-order mode in the transversal direction. The deformation was clearly larger on the east side than on the west side; the modal amplitude on the roof was 1.7 times larger at location NE than at location NW. Characteristically, the torsional motion was clearly coupled in the translational mode. Mode II (1.51 Hz) was the first-order mode in the longitudinal direction. The torsional motion was coupled in the translational mode, although it did not seem to be clear as mode I. Mode III (2.23 Hz) was the first-order torsional mode. Mode IV (3.97 Hz) was the second-order mode in the longitudinal direction; however, it seemed to be coupled with the torsional motion. The three-dimensional mode of mode V (4.96 Hz) seemed to be the second-order torsional mode. It can be explained from the components of mode shapes at location SW and NW, which moved in the opposite direction to location NE. In addition, the deformation is larger on the west side than on the east side. Mode VI (6.71 Hz) was clearly the third-order mode in the longitudinal direction. In contrast to the other modes, the torsional deformation could not be found in the mode. The third-floor modes were different from each other at the three locations.

The second- and third-order modes in the transversal direction could not be identified through this method. The mode shape of location SW around the third-floor in the longitudinal direction was different from that of other locations on mode IV and VI. These causes are currently under investigation.

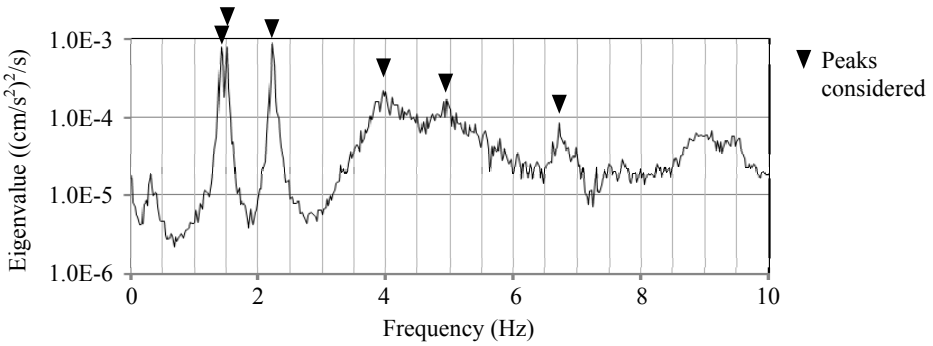

Figure 5. Eigenvalues of PSD matrix of response

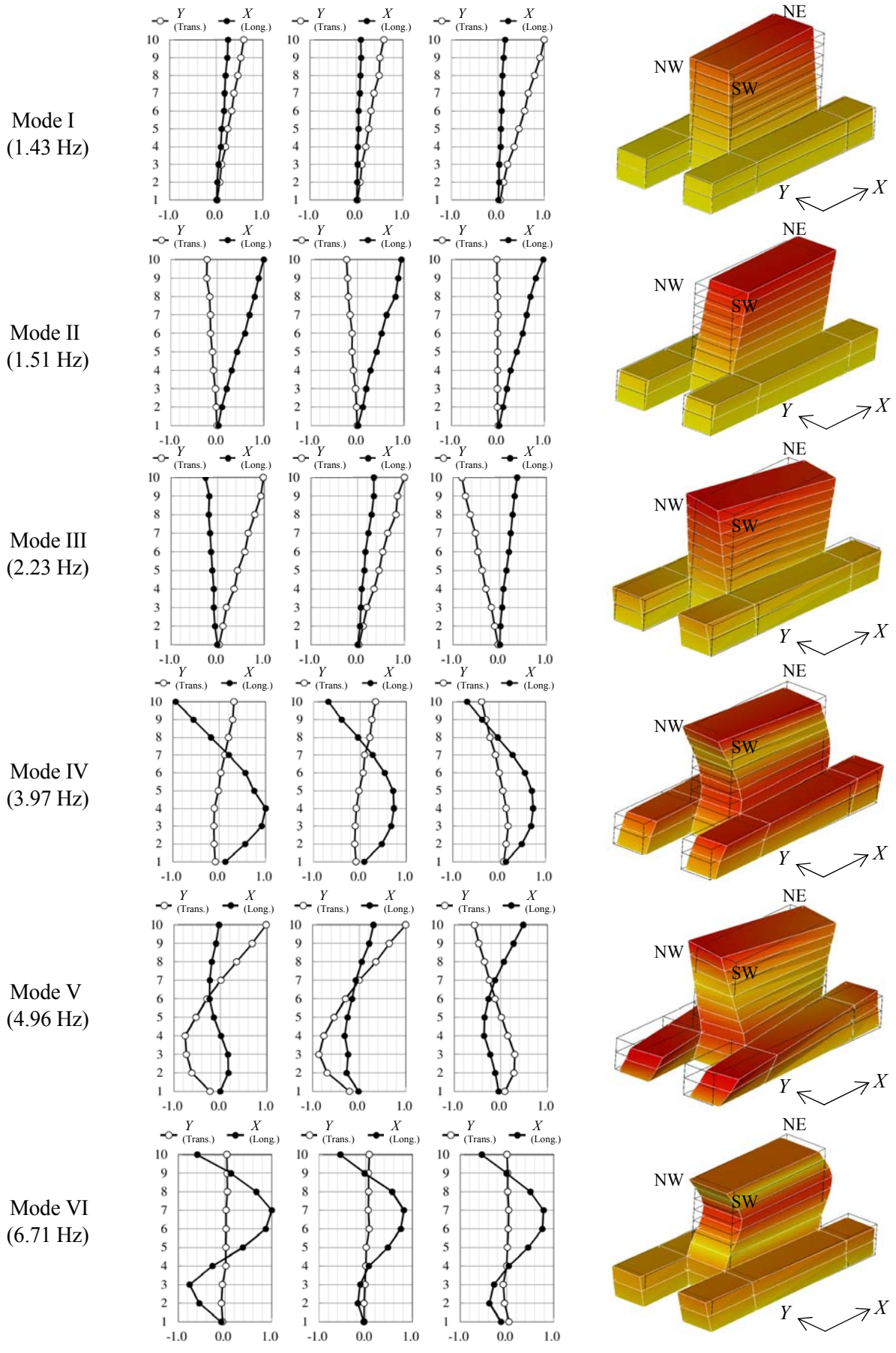

Figure 6. Identified modes at three locations (SW, NW, NE) and three-dimensional mode

(*ii*) *Torsional component found in translational mode*

As noted previously, the first- and second-order translational modes (modes I, II, and IV) seemed to be coupled with the torsional motion. The characteristics were roughly quantified by using the *i*th mode vector at the center of mass, which was represented by $\{u_X^C, u_Y^C, u_R^C\}^T$. As described in Fig. 7, $\boldsymbol{U_T}$ denotes the maximum *i*th mode value at the center of mass ($_iu_X^C$ *or* $_iu_Y^C$), and $\boldsymbol{U_R}$ denotes the torsional deformation expressed as the quasi-transversal deformation at the edge of the floor. Table 1 lists the ratios of $\boldsymbol{U_R}$ to $\boldsymbol{U_T}$ ($\boldsymbol{U_R}/\boldsymbol{U_T}$) for each translational mode. $\boldsymbol{U_R}/\boldsymbol{U_T}$ was unusually large for mode I. This indicates a stiffness unbalance in the transversal direction, and the effect likely appeared in the first-order translational mode. $\boldsymbol{U_R}/\boldsymbol{U_T}$ was variable for each mode.

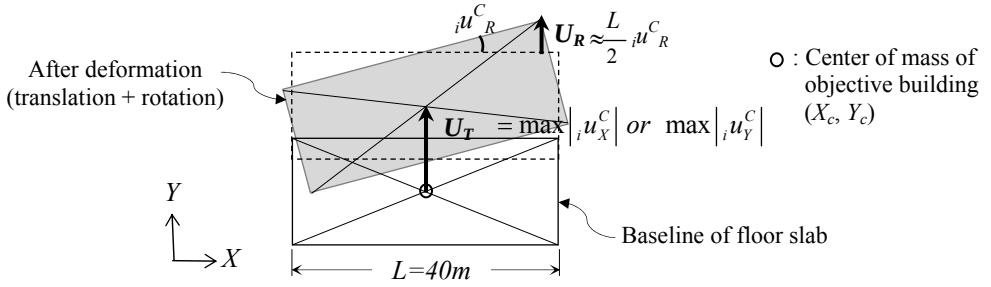

Figure 7. Illustration of plane vibration model (e.g. vibration in *Y*-direction)

Table 1. Ratio of torsional component to translational component

	Mode I	Mode II	Mode IV	Mode VI
Natural frequency	1.43 Hz	1.51 Hz	3.97 Hz	6.71 Hz
Ratio $\boldsymbol{U_R}/\boldsymbol{U_T}$	25.5%	10.0%	17.8%	3.6%

(*iii*) *Modal deformation ratio between floors*

The amount of lateral deformation generally changes with height. To quantify the change, the slope of the *i*th mode was introduced. This is expressed as the *i*th modal deformation ratio $_i\delta_k^j$ at the *j*th- floor for component *k* and is calculated from the differences in mode values between the (*j* + 1)th- floor $_iu_k^C\big|_{j+1}$ and the *j*th- floor $_iu_k^C\big|_j$ by

$$_i\delta_k^j = \left({}_iu_k^C\big|_{j+1} - {}_iu_k^C\big|_j \right) / h_j \tag{3.10}$$

where h_j is the story height between the (*j*+1)th- floor and the *j*th- floor. The heights were h_1 = 6.15 m, h_2 = 4.3 m, h_3 = 3.8 m, $h_4 \sim h_8$ = 3.3 m, and h_9 = 3.42 m.

Fig. 8 shows the identified mode shapes $\{u_X^C, u_Y^C, u_R^C\}^T$ for the most dominant component in each mode (left) and its deformation ratio $_i\delta_k^j$ (right). With respect to the translational modes, not only the dominant component but also its perpendicular component are shown as a reference. Each mode was normalized so that the maximum value was equal to 1.0. Considering that (1) the arrangement of structural members of the upper floors were uniform except for the third floor and (2) the section sizes of each structural member gradually became smaller at higher floors, the distribution of $_i\delta_k^j$ is expected to change with height uniformly above the third floor. However, the deformation ratio $_i\delta_k^j$ changed irregularly above the third floor for modes I, II, and III. Thus, the irregular pattern of $_i\delta_k^j$ may be related to structural damage from earthquakes.

Note the analogy between the distribution patterns of $_1\delta_X^j$ (mode I) and $_3\delta_R^j$ (mode III). Both took larger values than the other floors at *j* = 3, 5, and 7. Meanwhile, $_2\delta_Y^j$ (mode II) took a larger value than the other floors at *j* = 5 and 7 and also had an irregular pattern. On the other hand, the patterns of $_4\delta_X^j$ (mode IV), $_5\delta_R^j$ (mode V), and $_6\delta_X^j$ (mode VI) were more regular than those of the first-order modes. Thus, the tendency of the deformation ratio pattern seems to depend on the mode.

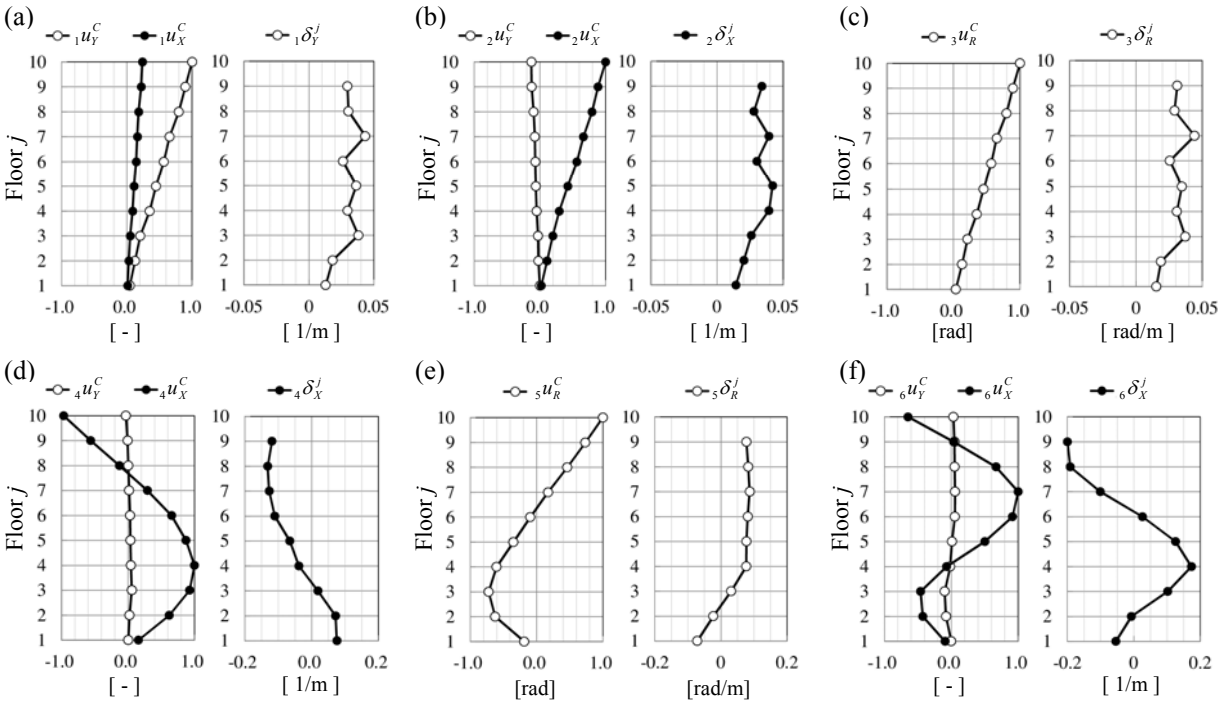

Figure 8. Mode shapes and modal deformation ratio at center of mass: (a) mode I, (b) mode II, (c) mode III, (d) mode IV, (e) mode V, and (f) mode VI

DISCUSSION

(*i*) *Changes in natural frequency based on ambient vibration*

After construction was completed, the ambient vibrations of the building were tested more than 10 times (Motosaka et al., 2012). Motosaka et al. (2002) revealed that the stiffness of the building greatly decreased after the 1978 Miyagiken-Oki earthquake and recovered after the seismic retrofitting of 2000-2001. Table 2 presents the changes in natural frequency of the first-order mode f_1 in the translational and torsional directions based on ambient vibration measurements since 2000 (measurement period No. 1). Fig. 9 shows the changes in frequencies listed in Table 2 by percentage after retrofitting in 2001 (No. 2). From the retrofitting in 2001 (No. 2) to March 9, 2011 (No. 3), the building was subjected to large earthquakes, and f_1 had already decreased during this time. The decrease in frequency was larger in the longitudinal direction (13%) than in the transversal direction (7%).

After the 2011 Tohoku earthquake on March 19, 2011 (No. 5), f_1 decreased by 26% and 13% in the transversal and longitudinal directions, respectively. The change in the transversal direction was much larger than in the longitudinal direction, and this result coincided with the damage situation of the building. Although the largest aftershock occurred on April 7, f_1 on May 3, 2011 (No. 6) did not change from March 19 (No.5). After that, the frequencies became higher because of the emergency rehabilitation in May, 2011 and the removal of furniture and materials out of the building, which lightened of the building weight. The natural frequencies after March 11, 2011 (No. 4) in the transversal and longitudinal directions decreased by 13% and 7%, respectively, by September 13, 2011 (No. 8) and 10% and 5%, respectively, by January 20, 2012 (No. 9).

According to Fig. 9, the changes in the frequency ratio for the torsional mode were clearly analogous to those in the translational direction. Although f_1 was not measured for the torsional mode after 2001 for about ten years, the changes in f_1 for the torsional mode should have been the same as those for the translational modes. In addition, the analogous results of ${}_1\delta_Y^j$ (mode I) and ${}_3\delta_R^j$ (mode III) in Fig. 8 suggest that f_1 for the torsional mode traced the same changes as that for the transversal mode over the years.

Table 2. Changes in natural frequency based on ambient vibration measurements

Measurement period		First-order natural frequency f_1(Hz)		
		Translational mode		Torsional mode
		Y-direction (transversal)	*X*-direction (longitudinal)	
No. 1	In 2000, before retrofitting (Motosaka et al., 2002)	1.48	1.54	2.20
Seismic retrofitting from September 2000 to March 2001				
No. 2	In 2001, after retrofitting (Motosaka et al., 2002)	1.74	1.85	2.61
Earthquakes (May 2003, July 2003 and 2008)				
No. 3	March 9, 2011 (Motosaka et al., 2012)	1.61	1.61	-
No. 4	March 11, 2011 (Motosaka et al., 2012)	1.61	1.61	-
2011 Tohoku earthquake				
No. 5	March 19, 2011 (Motosaka et al., 2012)	1.17	1.37	-
After shock of 2011 Tohoku earthquake				
No. 6	May 3, 2011 (Motosaka et al., 2012)	1.17	1.37	-
Emergency rehabilitation				
No. 7	May 31, 2011 (Motosaka et al., 2012)	1.37	1.48	-
No. 8	September 13, 2011	1.38	1.48	2.15
Removal of furniture and materials out of building				
No. 9	January 20, 2012	1.43	1.51	2.23

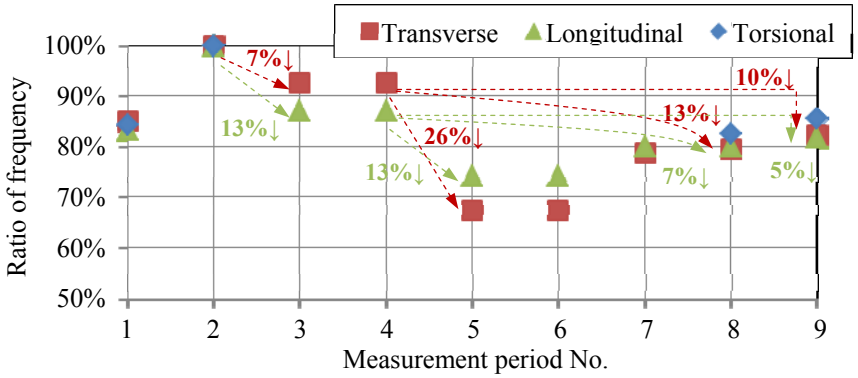

Figure 9. Changes in natural frequency based on ambient vibration measurements (represented by percentage based on measurement period No. 2)

(*ii*) *Damage location from modal properties*

The relationship between modal properties and damaged part was examined mainly based on the ratios U_R/U_T in Table 1 and the changes in the natural frequency as observed in this study and previous studies.

First, changes in the stiffness unbalance of the building were reviewed as follows. Based on the initial building design, the earthquake-resistant elements were mainly allocated to the north side of the floors; that is, the stiffness of the building was unbalanced only in the longitudinal direction. The eccentricity of the stiffness allowed the building to vibrate in the rotational direction with longitudinal vibrations; Shiga et al. (1973) conducted a forced vibration test just after the completion of construction and demonstrated this vibrational characteristic. In the seismic retrofitting of 2000-2001, steel braces were installed on the side in the longitudinal direction; Motosaka et al. (2002) performed the forced vibration test before and after the retrofitting and demonstrated that the ratio of rotational deformation to the first translational mode was reduced after the retrofitting. Therefore, there would have been almost no stiffness unbalance for both directions after the seismic retrofitting of 2000-2001. In this study, however, the obtained U_R/U_T for mode I was 25.5% which was much larger than that of other translational modes. Considering the reduction percentage of the rotational component in the

transversal direction after the seismic retrofitting (Motosaka et al., 2002), the large value of U_R/U_T appears to have been caused by the main shock of the 2011 Tohoku earthquake.

The characteristics obtained from identified modal properties are summarized as follows. (1) The decreasing rate of the natural frequency f_1 in the transversal direction was larger than that in the longitudinal direction after the 2011 Tohoku earthquake. (2) The distribution of the modal deformation ratio δ for mode I (transversal mode) was analogous to that for Mode III (torsional mode), and the ratio δ for both modes jumped at $j = 3$, which indicates the deformation clearly change from the third floor in the transversal direction. (3) The deformation in mode I was larger on the east side than on the west side. In particular, the modal amplitude on the roof was 1.7 times larger at location NE than at location NW. (4) The main shock decreased f_1 in the transversal direction from 1.61 Hz to 1.17 Hz. Meanwhile, the emergency rehabilitation caused f_1 in the transversal direction to jump from 1.17 Hz to 1.37 Hz; the ratio of the recovery frequency corresponds to nearly half of the decrease in frequency. Considering that the contents of the emergency rehabilitation were strengthening the four corner columns and installation of reinforced concrete shear walls in the corner frames, the stiffness of the side wall appears to be dominated in the total stiffness of the building in the transversal direction.

From these results, it is concluded that the increased eccentricity of the stiffness in the transversal direction was a result of the 2011 Tohoku earthquake and more severe damage occurred on east side of the gable wall around the third floor.

CONCLUSION

This study considered the damage detection problem by using a nine-story SRC building severely damaged by the 2011 Tohoku earthquake. Simultaneous high-density measurement of the ambient vibration was conducted, and modal parameters were identified from the ambient vibration records by using the FDD technique. The three-dimensional mode shapes were used to obtain the characteristics of the torsional vibration. Focusing on the changes in the natural frequency over time, the mode shape, and the modal deformation ratio, seismic damage of the building are discussed.

1) The natural frequency of the first-order mode f_1 just before the Tohoku earthquake was 1.61 Hz in the transversal and longitudinal directions. It respectively fell to 1.17 Hz and 1.37 Hz in the transversal and longitudinal directions after the main shock, the decrease in frequency was much larger in the transversal direction than in the longitudinal direction. After emergency rehabilitation, they recovered to 1.37 Hz and 1.48 Hz, respectively. The effect of damage that had not been repaired was supposed to be apparent in these frequencies.
2) Some of the identified translational modes seemed to be coupled with the torsional motion. In particular, the ratio of torsional components to translational components exceeded 25% in the first-order mode in the transversal direction. Considering that there was almost no eccentricity in the stiffness distribution after the 2000-2001 seismic retrofitting, the increased eccentricity in the transversal direction was apparently caused by the main shock of the 2011 Tohoku earthquake.
3) The distribution of the modal deformation ratio for the first transversal mode was analogous to that of the first torsional mode. The ratio for both modes jumped at the third floor. In addition, the distribution in the first translational modes and first torsional mode were irregular above the third floor. Although these tendencies were not clearly found in the higher-order of modes, they may be associated with the seismic damage.
4) The information obtained from the torsional vibrational characteristics can be a useful damage indicator. When measuring the ambient vibration for damage detection, it is preferable to locate sensors so that the torsional vibration property can be obtained.

REFERENCES

Au SK and Zhang FL (2011) "On assessing the posterior mode shape uncertainty in ambient modal identification", *Probabilistic Enginnering Mechanics*, 26, 427-434.

Belleri A, Moaveni B, Restrepo JI (2014), "Damage assessment through structural identification of a three-story large-scale precast concrete structure", *Earthquake Engineering Struct. Dyn.*, 43, 61-76.

Brincker R, Zhang L, Andersen P (2001) "Modal identification of output-only systems using frequency domain decomposition", *Smart Material and Structures,* 10, 441-445.

Ghahari SF, Abazarsa F, Ghannad MA, Taciroglu E (2013) "Response-only modal identification of structures using strong motion data" *Earthquake Engineering Struct. Dyn.*, 42, 1221-1242.

Hamamoto T and Kondo I (1999) "Two-stage damage detection of eccentric multistory buildings using vertical and horizontal searching", *Journal of Structural and Construction Engineering*, 519, 21-28. (Japanese)

Hirabayashi M, Kimura H, Ishikawa Y, Tanabe Y, Maeda M and Ichinose, T (2012) "Investigation on building in Tohoku University damaged by the 2011 Great East Japan Earthquake Part 4: Study on building of civil engineering and architecture by earthquake response analysis (2)", Summaries of Technical Papers of Annual Meeting , Japan, 13-16. (Japanese)

Hsu TY and Loh CH (2013) "A frequency response function change method for damage localization and quantification in a shear building under ground excitation", *Earthquake Engineering Struct. Dyn.*, 42, 653-668.

Iiyama K and Kurita S (2013) "Theoretical background of modal identification technique using spectrum decomposition taking account of close modes", *Journal of Structural and Construction Engineering*, 684, 271-280. (Japanese)

Kim JT (2002) "Improved damage identification method based on modal information", *Journal of Sound and Vibration*, 252(2), 223-238.

Moaveni B, He X, Conte JP, Restrepo JI (2010) "Damage identification study of a seven-story full-scale building slice tested on the UCSD-NEES shake table", *Structural Safety*, 32, 347-356.

Motosaka M, Suzuki H, Sato T (2002) "Evaluation of seismic damage and reinforcement effects of an existing building based on forced vibration tests before and after the reinforcement work", *The Earthquake Engineering Symposium Proceedings* , Japan, 11, 2015-2020. (Japanese)

Motosaka M, Tsamba T, Yoshida K, Mitsuji K (2012) "Long-term monitoring of amplitude dependent dynamics characteristics of a damaged building during the 2011 Tohoku earthquake", *Journal of JAEE*, 12, 5, 117-132. (Japanese)

Nakamura M and Yasui Y (1999) "Damage evaluation of a steel structure subjected to strong earthquake motion based on ambient vibration measurement", *Journal of Structural and Construction Engineering*, 517, 61-68. (Japanese)

Omrani R, Hudson RE, Taciroglu E (2012) "Story-by-story estimation of the stiffness parameters of laterally-torsionally coupled buildings using forced or ambient vibration data: I. Formulation and verification", *Earthquake Engineering Struct. Dyn.*, 41, 1609-1634.

Shiga T, Shibata A, Shibuya J (1973) "Dynamic properties and earthquake response of a 9 story reinforced concrete building", *Proc. 5th WCEE*, Roma, 2680-2683.

Strauss A, Frangopol DM, F.ASCE, Bergmeister K (2010), "Assessment of existing structure based on identification", *J. Struct. Eng.*, 136, 86-97.

Teughels A, Maeck J, Roeck GD (2002) "Damage assessment by FE model updating using damage functions", *Computers and Structures*, 80, 1869-1879.

Tsamba T and Motosaka M (2011) "Investigation of dynamic behavior of a damaged 9-story building during the 2011 off the Pacific Coast Tohoku Earthquake", *JAEE Annual Conference*, 44-45.

Xu ZD and Wu KY (2012) "Damage detection for space truss structures based on strain mode under ambient excitation", *J. Eng. Mech.*, 138, 1215-1223.

Yang Y and Nagarajaiah, S (2013) "Blind modal identification of output-only structures in time-domain based on complexity pursuit", *Earthquake Engineering Struct. Dyn.*, 42, 1885-1905.